Available online at www.sciencedirect.com

ScienceDirect

materialstoday: PROCEEDINGS

ICKEM 2020 Materials Today Proceedings

In situ SEM analysis of surface oxidation mechanisms in carbon steel during vacuum heat treatment

Rhiannon Heard, Clive R. Siviour, Kalin Dragnevski

Solid Mechanics and Materials Group, Department of Engineering Science, University of Oxford, Parks Road, Oxford, OX1 3PJ

Abstract

Understanding surface effects, such as oxidation, that occur during the heat treatment of steels is vital in producing desirable mechanical properties. To mitigate against thermal oxidation, heat treatments are often conducted in a 'fine' vacuum (~10^{-4} mbar); however, studies have shown that even at these vacuum levels, oxidation occurs. To further understand this behaviour, an alternative *in situ* Scanning Electron Microscopy approach, facilitated by a novel heat stage, has been used to study the surface morphology of carbon steel during thermal oxidation. The data provide insight into the surface formation of oxidation under fine vacuum conditions, demonstrating that the process begins with the generation of thermally etched grain boundaries, where initial oxidation is focussed, followed by the formation of oxide scales across individual grains. Eventually these individual scales agglomerate to form a continuous oxide layer. The data further suggest that these oxide layers are likely to be predominantly wüstite. The surface data also indicate an absence of blistering, commonly observed on the steel surface at the these temperatures and timescales. The lack of blisters both *in situ* and ex-situ is thought to be attributed to an absence of a gaseous environment preventing blister formation.

Keywords: High-Temperature imaging, SEM, Oxidation, carbon-steel;

1. Introduction

The heat treatment of carbon steels is applied in order to form preferential microstructures, which in turn produce desirable mechanical properties [1]. The formation of oxide layers during heat treatment in air and oxygen rich environments, known as thermal oxidation, is common, and impacts the resulting surface properties of the carbon steel. Studies of the oxidized carbon steel surface confirm that theories concerning the kinetics and mechanisms with regards to rate are valid and well understood [2]. Cross sections taken of oxidised carbon steel surfaces using Secondary Electron and Atomic Force Microscopy show that there are three main oxide layers, which form during heat treatments of carbon steel: wüstite, haematite and magnetite. The exact combination and composition of these layers is dependent on time, temperature, oxidation level and pressure. For short time periods of heating, formation of layers is not dissimilar to that occurring in pure iron, generating an initial wüstite scale layer, and after a longer period leading to layers of haematite and magnetite. During further prolonged heating periods, wüstite scales are less defined and eventually the scales interfere with each other; at temperatures of 850 °C and above this eventually results in blistering [3].

Blistering is the appearance of pockmarks or irregular shapes on the surface of thermally oxidised carbon steel formed of a cavity between the scale and substrate composed of haematite and magnetite layers with some wüstite [4].

Studies indicate that a gas phase, produced either from carbon oxidation or inert gas in the surrounding atmosphere [5], is necessary for blistering to occur [3]. Without the gas phase, it is considered after blister formation the cavity may be healed by annihilation mechanisms (creep / plastic flow of the scale) [6]. This healing mechanism is thought to explain why there are conflicting data on blistering behaviour [4], [5]: blisters may have formed during oxidation but have subsequently healed. Additionally, oxidation surfaces produced under low gas atmospheres also show an absence of blisters, again thought to be due to the lack of gas available to sustain blister formation during the cooling process, resulting in healing. However, the lack of *in situ* data means the exact blister formation process is not fully understood, and there is little evidence post cooling of healed blisters.

To mitigate against the formation of these oxide layers, carbon steels are often heat treated under what is commonly described as 'fine' vacuum (~ 10^{-4} mbar) [7]. However, it has been documented that some oxidation of the surface can still occur even at these vacuum levels [8]. This is due to the fine vacuum environment being formed in a chamber that has initially contained air; as such, sufficient levels of oxygen remain to cause oxidation during the heat treatment process. However, under such conditions, oxidation has a significantly slower initial rate compared to that in pure oxygen or air [9]. Additionally, the oxidation scale composition is heavily dependent on pressure and oxygen levels, identified using a combination of neutron diffraction *in situ* studies and electron spectroscopy. In particular, *in situ* neutron diffraction measurements have provided compositional data that indicate that under low oxygen / air pressures above temperatures of 570 °C, the dominant layer is wüstite [4]. To compliment the compositional *in situ* data available, attempts have been made to understand the morphology of steel formed *in situ* [10] [11]. One such study focussed on the formation of oxidation of carbon steel within the first 30 seconds of hot-rolling using a CCD camera. This demonstrated that the grain boundaries appeared visible following exposure to high temperature, indicating that diffusion through steel grain boundaries may influence oxide formation [11].

From the literature, it is clear there is a lack of data documenting the morphological processes by which oxide scales form on carbon steels, particularly under a vacuum environment and during complete heat treatment cycles. Thus, this paper uses high temperature *in situ* Scanning Electron Microscopy to capture the formation of surface oxidation during the heat treatment of carbon steels under a 'fine' vacuum environment. The resulting data aims to provide further fundamental understanding of the formation of the carbon steel oxide layer.

2. Materials & Methodology

This research investigated the oxidation of carbon steel during heat treatment in a 'fine' vacuum environment. The study uses cylindrical samples of 0.4% wt. carbon steel of 8 mm diameter by 1 mm thickness. Samples were heated at a rate of 1 °C/s up to 850 °C and held for four hours, to maximise the oxidation, and subsequently cooled over a period of one hour. The heat treatment temperature of 850 °C was chosen as this is the standard mid-range temperature for heat treatment of 0.4% wt. carbon steels [12]. The complete heat treatment cycle was conducted in a Carl Zeiss Evo Scanning Electron Microscope (SEM) with LAB6 crystal source operating at 20 kV. The SEM sample chamber was kept under a vacuum of approximately $1x10^{-4}$ mbar during the complete heat treatment, as this is within the 'fine' vacuum range for heat treatment of steels [7]. To conduct the heat treatment *in situ*, a novel heat stage, developed in collaboration with Deben UK Ltd and comprising of a molybdenum button heater with the capability to allow imaging up to 920 °C without the need for shielding, was used [13]. Prior to heat treatment, the sample surface was ground using progressively finer silicon carbide papers and polished using diamond solution and subsequently colloidal silica, as is standard practice for oxidation experiments [2]. During the heat treatment process, secondary electron (SE) images were captured at frequent time intervals at magnifications of 500x, 1.5kx and 2kx. To evaluate the compositional changes to the sample surface, EDX scans were taken before and after the heat treatment. EDX data was captured for an area of 100 × 100 µm over 200 frames. Post heat treatment optical images were also captured of the thermally etched surface using an Alicona Profilometer.

3. Results & Discussion

An alternative approach has been applied to study the surface morphology of oxidation using *in situ* SEM imaging at high temperature. Before examination and analysis of the *in situ* data were conducted, EDX data were taken pre and post heating: firstly to confirm oxidation had occurred and secondly to identify which morphological features represented the oxidised steel. Figure 1a shows the typical spectrum of a steel specimen before heat treatment, where it is clearly observed that there is no oxygen present on the surface. In contrast, figure 1b shows a significant level of oxidation post heat treatment, with oxygen levels in the region of 16wt%.

To correlate the morphologies observed in the SE images with composition, EDX maps pre and post heating were examined; see figure 2 and 3 respectively. Figure 2 shows the maps pre heating and identifies the large nodule shown in the SE image as a concentrated area of carbon precipitate (circled in black) and the smaller raised areas as other alloying elements (circled in red). The maps obtained pre heating indicated that no oxygen was present. Examination of the composition post heating, figure 3a, shows two distinct types of morphology. The morphology is compared to the two main elements identified on the surface; iron and oxygen, figure 3b. From these it can be seen that the lighter white areas in the SE image are predominantly oxygen (yellow), whilst the darker areas in the SE image are identified as iron (green). With this compositional information, the SE images can be analysed with the ease of distinguishing oxygen formation from the steel surface.

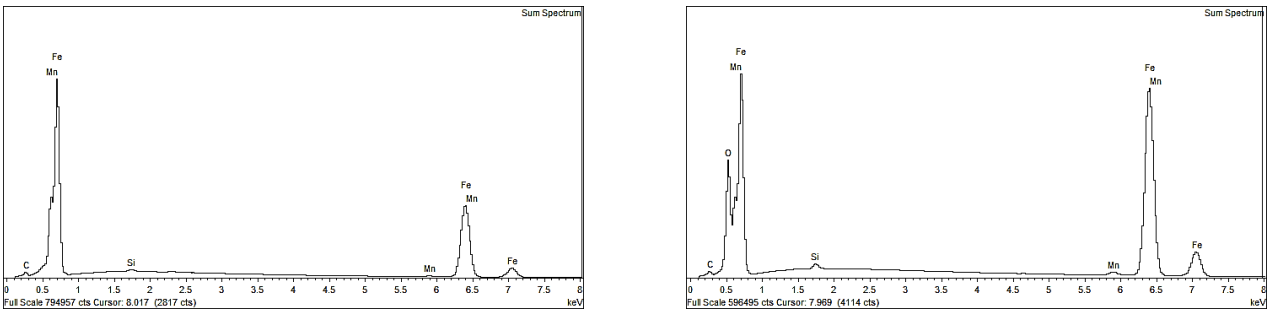

(a) (b)

Figure 1: EDX spectra showing (a) no detectable oxygen before heating of the polished carbon steel sample and (b) oxygen present after heating.

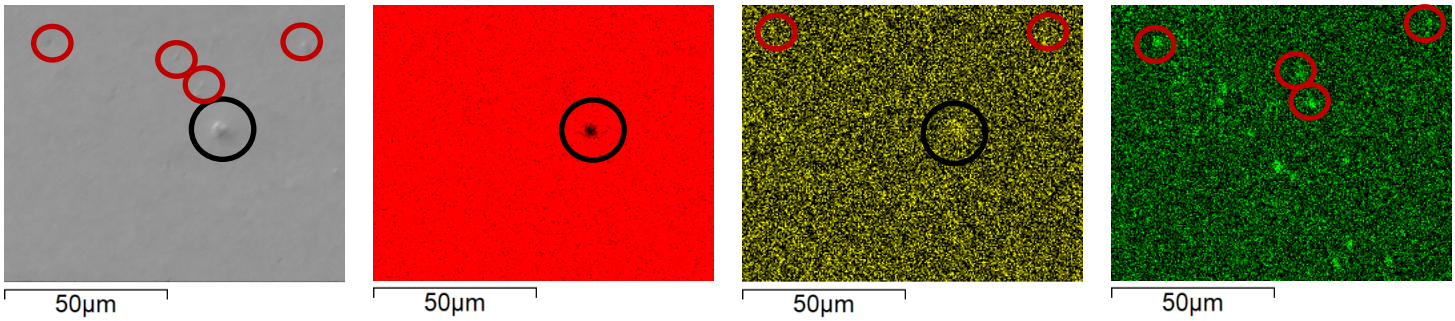

(a) (b) (c) (d)

Figure 2: EDX composition maps of steel pre heat treatment. (a) SE imaged area used to capture EDX maps corresponding to (b) iron, (c) carbon and (d) manganese. The nodule in the SE image circled in black is a carbon precipitate, as indicated by the absence of iron in (b) and concentrated presence of carbon in (c). The red circles in (a) indicate a combination of carbon (c) and other negligible alloying elements such as manganese (d).

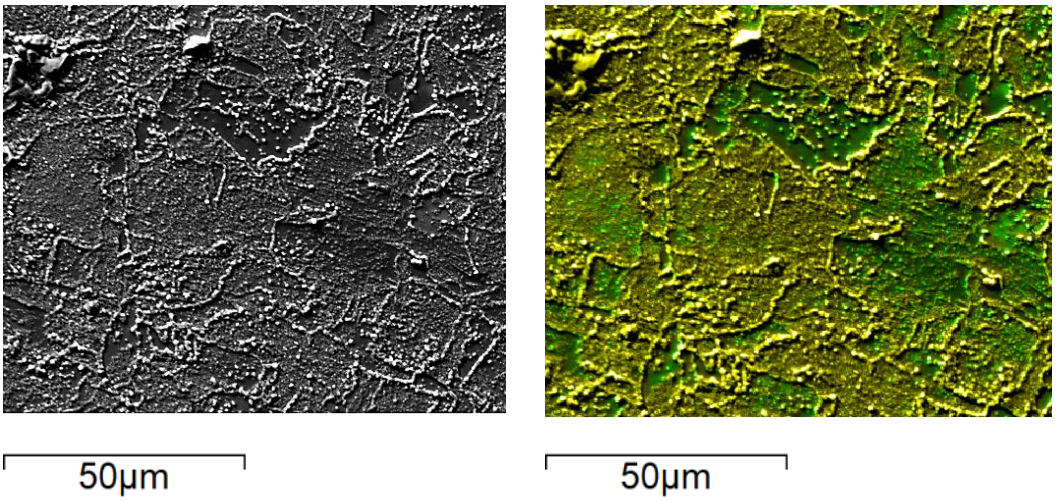

(a) (b)

Figure 3: EDX composition maps of steel post heat treatment of the dominant surface compositions of oxygen and iron. (a) SE imaged area used to capture the EDX data showing two distinctive morphologies. (b) Combined composition EDX map showing iron (green) and oxygen (yellow) corresponding to dark and lighter areas of SE image respectively.

To observe the formation of the oxide layer, as confirmed by the EDX data, SE images were captured *in situ*. The results for the heat treatment carried out are presented in figure 4, which shows a sequence of images with respective times at 850 °C (figure 4a – 4i) and at room temperature post heating (figure 4j). Figure 4a shows the SE image of the carbon steel surface once the required heat treatment temperature of 850 °C was reached. Here, the initial formation of the outline of grain boundaries is observed; arrows show clear points where the grain boundary grooves begin to emerge. The grain boundaries are visible due to a phenomenon known as "thermal etching" which is a common formation when a polished metallic surface is exposed to elevated temperatures [14]. Thermal etching affects the grain boundaries that impinge on the specimen surface; because of equilibration of the triple junction between the grain boundary and the free surface, the surrounding specimen surface rises away from the boundary [15]. The SE image also shows the beginnings of possible oxidation in the two to three highlighted white dots. The initial areas of oxidation occur where there are raised topography, which are identified as concentrated areas of carbon in the EDX maps in figure 2. After 10 minutes of heating, figure 4b, there appears to be minimal further oxidation. However, there is a significant change in the ratio between the darker and lighter areas of the image. The image colouring is a uniform grayscale tone; this indicates the phase change is likely complete and the imaged area is fully austenitic. EBSD studies on carbon steel during heat treatment have shown that the phase change from ferrite-austenite to pure austenite doesn't always happen immediately despite the surface reaching the fully austenitic temperature [13][16]. Furthermore, the different grayscale levels of the image can indicate a difference in phase [17].

Figure 4c shows that after 20 minutes of heating at 850 °C there are almost no dark areas remaining, signifying that the phase change is complete. The first signs of oxidation of the general steel surface rather than just specific points can also be seen. In this figure, the sides of etched grain boundaries appear slightly lighter in colour, indicating the initial formation of oxides (highlighted by the arrow). This becomes even more pronounced 5 minutes later, figure 4d, where multiple grain boundaries are showing signs of oxidation (white lines); this can be more clearly seen in the higher magnification image. From the *in situ* observations, it is evident that oxidation likely initially occurs along the grain boundary grooves rather than the surface, as thermal oxidation is a diffusion driven process and thus occurs on exposed surfaces [18]. The process of thermal etching forms newly exposed surfaces (along the grain boundaries), which will have a higher surface energy than the current sample surface. As a result of the higher surface energy, the

diffusion-driven oxidation process is more likely to happen along the boundary rather than on the original sample surface, which has a lower surface energy in comparison. The presence of oxidation within the grain boundary groove, figure 4d, is a phenomenon that has previously been documented in thin films [19].

Once the oxidation of the new grain boundary surface is complete, oxidation begins to occur on the original surface. Figure 4e, at nearly 1 hour of heating, shows this: the oxidation can be seen more clearly in the zoomed in area, with specific areas of clustered white nodules circled in red. The formation of the small white nodules represents the initial growth of the oxide scale, which appears to encroach on the grain from the edges of the grain boundaries towards the centre. This pattern continues to be the case after 1 hour 35 minutes, figure 4f. Figure 4g displays the surface after heating for over 2 hours at 850 °C, which shows some grains to be completely oxidised (highlighted in yellow). A similar rate of increasing oxidation by observation occurs through the 3rd (figure 4h) and 4th (figure 4i) hours of heating. After 4 hours most of the surface is covered in oxide scales, appearing to run along the grain boundaries, with some areas of oxide agglomeration. This surface appearance remains the same post cooling, figure 4j; although the scales are slightly clearer owing to the lack of light pollution, which can effect image quality at high temperature [13]. The surface shown in figure 4j is the morphology commonly imaged post heating ex-situ [20].

The observation of scale morphology over time documented during this *in situ* study may also provide an insight into the type of surface oxide that forms during heat treatment under 'fine' vacuum environment. Although this SEM/EDX approach does not determine the exact composition of the surface oxide layer, there are several factors suggesting that the dominant type of oxide is wüstite. Firstly, the scale formation with clearly defined boundaries, observed in this study, is common of the wüstite layer and is likely facilitated by the formation from edges to grain centre *in situ*. Additionally, when imaging the cross section of the oxidised surface of steels, SE images have shown the appearance of wüstite to be significantly lighter when compared to that of magnetite and haemetite [3]; the SE images documented in this study, see figure 3a, also show a large shade contrast between the steel and oxide layers. In further support of these morphological observations, studies documenting *in situ* neutron diffraction data taken during the heat treatment of steels under low pressure, show the dominant oxide layer is wüstite at 95 % compared to 4 % and 1 % of magnetite and haemetite respectively [9]. By considering the thermodynamics of oxide formation through examiation of the Ellingham diagram, a plot of the standard Gibbs free energy of reaction versus temperature used to compare the relative stabilities of each metal oxide based on the partial pressures of oxygen, it also suggests that wüstite is likely to be the dominant phase present [21]. Moreover, the diffisuion coefficient of iron in wustite is much greater than in magnetite or haemetite making it more likley to form in a lower oxygen environment or at lower temperatures [3], such as in this study. Nonetheless, the lack of blister formation may not be due to a lack of the magnetite and haemetite oxide layers. It is thought that the presence of a gaseous environment is also important for blisters to be observed on the oxidised surface post heating. However, the requirement for sufficient gas to be present is thought to be necessary to maintain a blister throughout the whole heat treatment cycle rather than for formation, otherwise it is expected the blister will heal / collapse [3]. Despite the heat treatment occuring at a temperature and over a time period where blistering would be expected to occur, neither formation nor healing / collapse of blisters is observed during the *in situ* heating process, suggesting that a sufficient level of gas (i.e. a non-vacuum environment) is also required for blisters to form.

Available online at www.sciencedirect.com

ScienceDirect

materialstoday: PROCEEDINGS

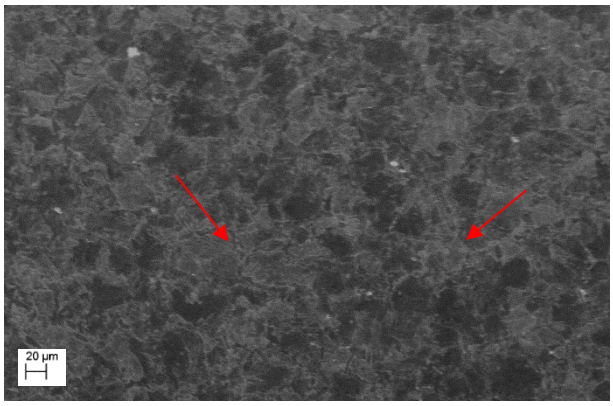

(a) T = 850 °C, t= 0 minutes

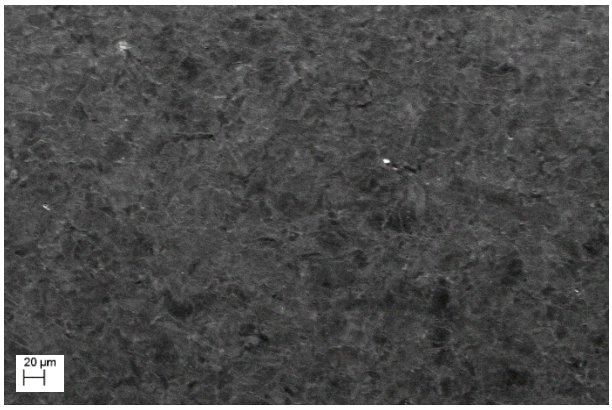

(b) T = 850 °C, t= 10 minutes

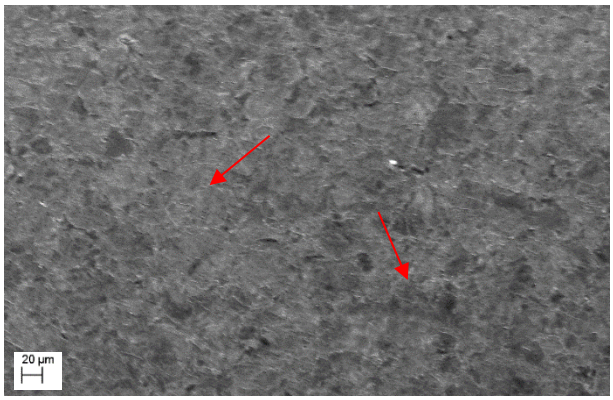

(c) T = 850 °C, t= 20 minutes

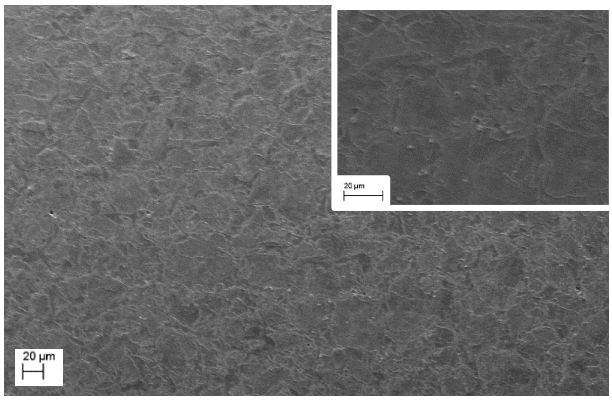

(d) T = 850 °C, t= 25 minutes

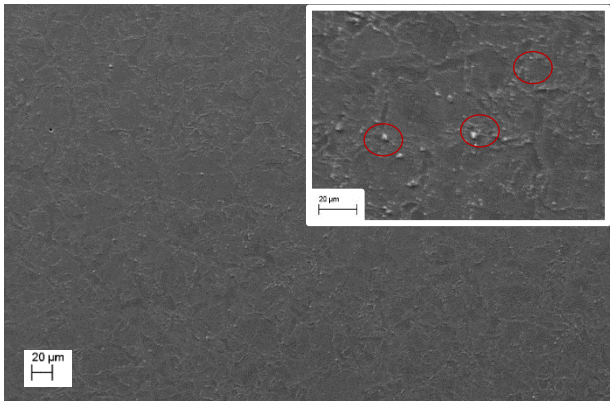

(e) T = 850 °C, t= 55 minutes

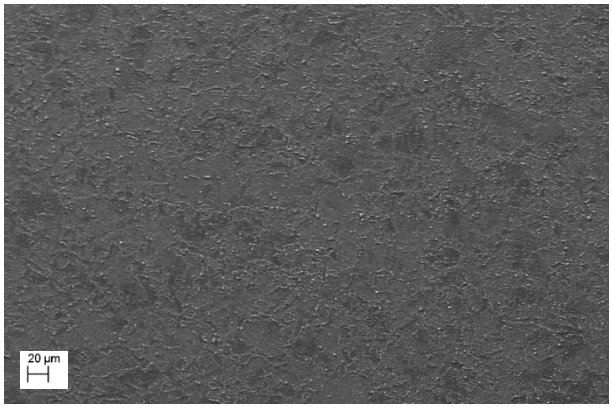

(f) T = 850 °C, t= 1 hour 35 minutes

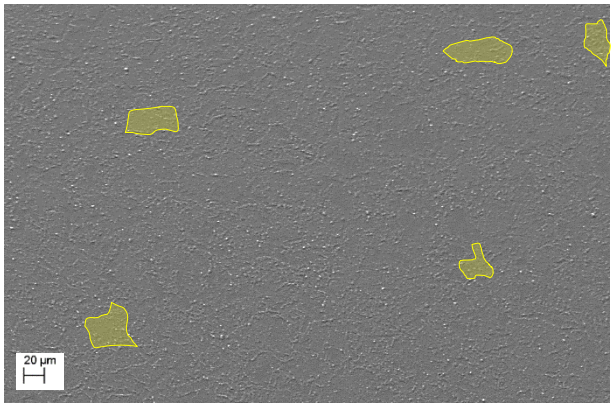

(g) T = 850 °C, t= 2hours 10 minutes

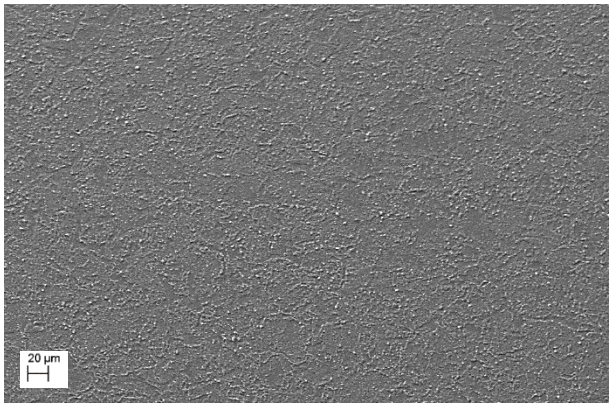

(h) T = 850 °C, t= 3 hours 15minutes

(i) T = 850 °C, t= 4 hours

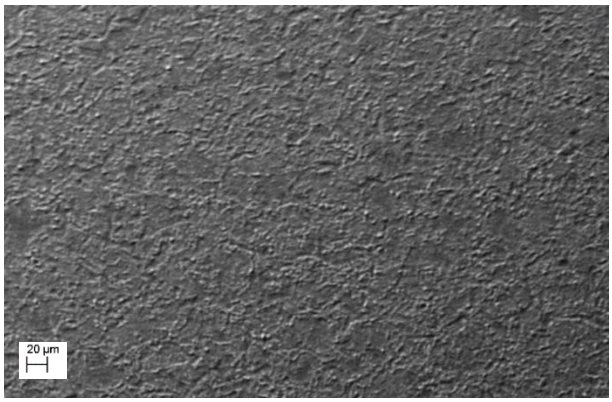

(j) T = Room temperature post cooling

Figure 4: *In situ* SE images showing the oxidation progression of the 4-hour heat treatment at 850 °C.

4. Conclusions

The research documented demonstrates an alternative *in situ* SEM approach to studying surface morphology of thermal oxidation. The data presented provide further insight into the formation process of oxide layers in carbon steels, which is affected by the presence of thermal etching and the subsequent agglomeration of oxide nodules, initially forming discrete oxide scales before eventually creating a more uniform oxide layer. Based on the morphology imaged in this study, combined with current data in the literature, it is thought this that the composition of the oxide layer formed under these conditions is predominantly wüstite. Finally, the lack of blistering present, which would be expected at these temperatures and time scales, indicates that either: multiple oxide layers are necessary for blistering to occur (indicating the lack of layers in this heat treatment), or a gaseous layer is required not only to support the blister and prevent collapse / healing but also to facilitate its formation in the first place. Hence, these findings highlight the benefit of capturing scale formation *in situ* to further the understanding of the mechanism by which iron-oxide layers form. This research forms part of a larger project studying surface effects during heat treatment of carbon steels.

Acknowledgements

The authors acknowledge funding from EPSRC under the iCASE scheme (Grant Number: EP/R512333/1; Award Reference: 1939581). We also thank Deben UK Ltd for providing both financial and technical support, Marzena

Tkaczyk for all her help operating the equipment in the LIMA microscopy suite and the technicians in the Solid Mechanics group workshop at Oxford University for producing specimens. Without the above mentioned, this research would not have been possible.

References

[1] D. Maritza, M. Cardona, J. Wongsa-ngam, and T. G. Langdon, "Microstructural evolution and microhardness in a low carbon steel processed by high-pressure torsion ϑ," *Integr. Med. Res.*, vol. 3, no. 4, pp. 344–348, 2014, doi: 10.1016/j.jmrt.2014.09.004.

[2] J. S. Sheasby, W. E. Boggs, and E. T. Turkdogan, "Scale growth on steels at 1200°C: rationale of rate and morphology," *Met. Sci.*, vol. 18, no. 3, pp. 1–10, 1984, doi: 10.1179/msc.1984.18.3.127.

[3] R. Y. Chen and W. Y. D. Yuen, "Review of the high-temperature oxidation of iron and carbon steels in air or oxygen," *Oxidation of Metals*, vol. 59, no. 5–6. pp. 433–468, Jun-2003, doi: 10.1023/A:1023685905159.

[4] F. Matsuno, "Blistering and Hydraulic Removability of Scale Films of Rimmed Steel At High Temperature.," *Tetsu To Hagane*, vol. 65, no. 6, pp. 599–607, 1979, doi: 10.2355/tetsutohagane1955.65.6_599.

[5] R. Griffiths, "The Blistering of Iron Oxide Scales and the Conditions for the Formation of a Non-adherent Scale," *J. iron steel Inst.*, vol. 130, 1934.

[6] H. Engell and F. Wever, "Über einige grundfragen der bildung und der haftung von zunder auf eisen," *Acta Metall.*, vol. 5, no. 12, pp. 695–702, Dec. 1957, doi: 10.1016/0001-6160(57)90071-8.

[7] "Vacuum heat treatment-Technical glossary-Bodycote Plc." [Online]. Available: https://www.bodycote.com/technical-glossary/vacuum-heat-treatment/. [Accessed: 29-Apr-2020].

[8] Y. Feng, H. Yu, Z. Luo, G. Xie, and R. Misra, "The Impact of Surface Treatment and Degree of Vacuum on the Interface and Mechanical Properties of Stainless Steel Clad Plate," *Materials (Basel).*, vol. 11, no. 9, p. 1489, Aug. 2018, doi: 10.3390/ma11091489.

[9] H. Abuluwefa, J. H. Root, R. I. L. Guthrie, and F. Ajersch, "Real-time observations of the oxidation of mild steel at high temperature by neutron diffraction," *Metall. Mater. Trans. B Process Metall. Mater. Process. Sci.*, vol. 27, no. 6, pp. 993–997, 1996, doi: 10.1007/s11663-996-0014-y.

[10] M. E. Story and B. A. Webler, "Evolution of Near-Surface Internal and External Oxide Morphology During High-Temperature Selective Oxidation of Steels," *JOM*, vol. 70, no. 7. Minerals, Metals and Materials Society, pp. 1225–1231, 01-Jul-2018, doi: 10.1007/s11837-018-2885-1.

[11] W. M. MELFO and R. J. DIPPENAAR, "*In situ* observations of early oxide formation in steel under hot-rolling conditions," *J. Microsc.*, vol. 225, no. 2, pp. 147–155, Feb. 2007, doi: 10.1111/j.1365-2818.2007.01726.x.

[12] P. H. Treating, "Fundamentals of the Heat Treating of Steel," 2006.

[13] E. W.-B. and K. D. Rhiannon Heard, John E. Huber, Clive Siviour, Gary Edwards, "An investigation into experimental in-situ SEM imaging at high temperature.," *Rev. Sci. Instrum.*, 2020.

[14] R. HEARD, K. I. DRAGNEVSKI, and C. R. SIVIOUR, "*In-situ* SEM observation of grain growth in the austenitic region of carbon steel using thermal etching," *J. Microsc.*, p. jmi.12894, Apr. 2020, doi: 10.1111/jmi.12894.

[15] W. W. Mullins, "Theory of Thermal Grooving," vol. 333, no. 1957, 1986, doi: 10.1063/1.1722742.

[16] H. Farahani, G. Zijlstra, M. G. Mecozzi, V. Ocelík, J. T. M. De Hosson, and S. Van Der Zwaag, "*In situ* High-Temperature EBSD and 3D Phase Field Studies of the Austenite-Ferrite Transformation in a Medium

Mn Steel," *Microsc. Microanal.*, pp. 639–655, 2019, doi: 10.1017/S143192761900031X.

[17] J. . Goldstein, D. E. Newbury, J. R. Micahel, N. W. W. Ritchie, J. H. J. Scott, and D. C. Joy, *Scanning Electron Microscopy and X-ray Microanalysis*, Fourth edi. Springer, 2018.

[18] H. D. Merchant, "Oxidation Kinetics of Iron-Carbon Base Alloys," 1970.

[19] Y. Zhang, A. Godfrey, and D. J. Jensen, "Kinetics of thermal grooving during low temperature recrystallization of pure aluminum," 2013, doi: 10.4028/www.scientific.net/MSF.753.117.

[20] A. A. El-Meligi, "Effect of heating rates on the formable oxide scale on a c-steel surface," *J. Mater. Sci. Technol.*, vol. 20, no. 5, 2004.

[21] C. P. Somrerk Chandra-ambhorrn, Thammaporn Thublaor, "Thermodynamics and Kinetics of the High Temperature Oxidation of Stainless Steels," *Solid State Phenom.*, vol. 300, pp. 1–24, 2020.